Electronic Supplementary Material (ESI) for Nanoscale Advances.

Mitigation of vacancy with ammonium salt-trapped ZIF-8 capsules for stable perovskite solar cells through simultaneous compensation and loss inhibition

Chi Li [#,†], Shanshan Guo[#,†], Jingan Chen [†], Zhibin Cheng[†], Mengqi Zhu[†], Jindan Zhang[*,†,‡] , Shengchang Xiang[†,‡], Zhangjing Zhang[*,†,‡]

[†]*College of Chemistry and Materials Science, Fujian Provincial Key Laboratory of Polymer Materials, Fujian Normal University, 32 Shangsan Road, Fuzhou 350007, China*

[‡]*State Key Laboratory of Structural Chemistry, Fujian Institute of Research on the Structure of Matter, Chinese Academy of Sciences, Fuzhou, Fujian 350002, PR China*

Supporting information

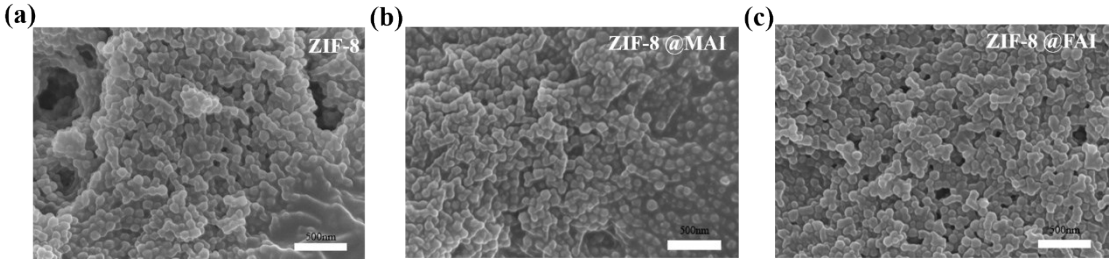

Fig. S1 SEM images of (a) ZIF-8; (b) ZIF-8@MAI; (c) ZIF-8@FAI

The SEM images of ZIF-8@MAI and ZIF-8@FAI revealed the homogenous distribution of synthesized ZIF-8.

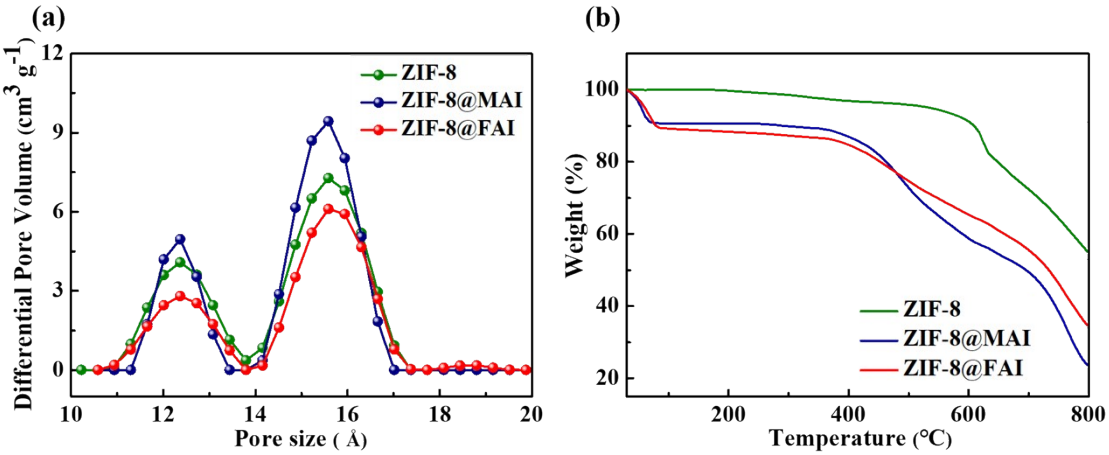

Fig. S2 (a) Pore size distribution and (b) (TGA) curves of ZIF-8, ZIF-8@MAI and ZIF-8@FAI.

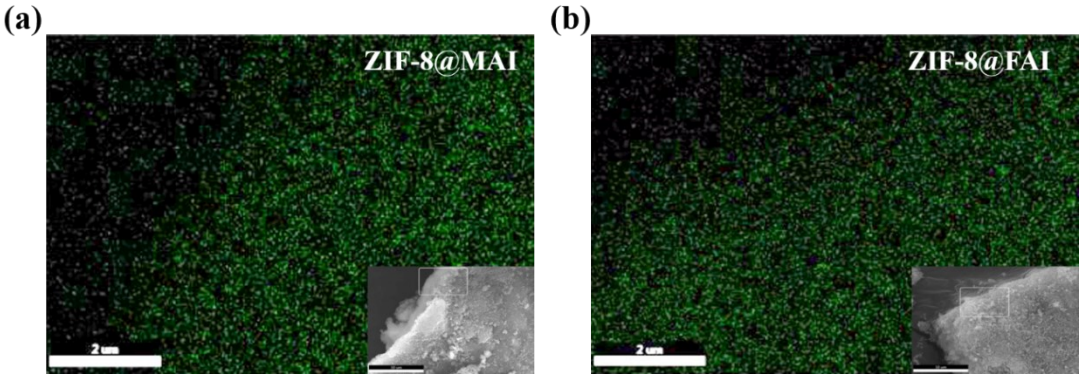

Fig. S3 I elemental maps (a) ZIF-8@MAI; (b) ZIF-8@FAI

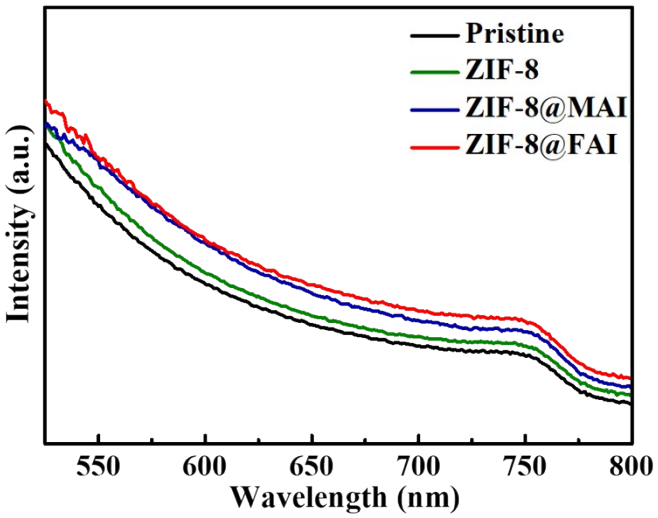

Fig. S4 UV–vis absorption of the device with ZIF-8, ZIF-8@MAI and ZIF-8@FAI modified and pristine.

To better understand the effects of ZIF-8, ZIF-8@MAI and ZIF-8@FAI passivation on the photophysical properties of perovskite films, we performed UV–vis absorption measurements for pristine and passivated perovskite films. As shown in Fig. R5, the UV-vis absorption spectra show a slight absorption enhancement over the region from 450 to 760 nm, which can be ascribed to the better crystallization and higher film quality. And further analysis based on the Tauc plots, as shown in Figure S5, the bandgaps were calculated to be 1.5685, 1.5635, 1.5634, and 1.5599 eV for Pristine, ZIF-8, ZIF-8@MAI and ZIF-8@FAI films, respectively. Results show that there is no noteworthy difference in absorption band edge, suggesting a negligible impact of ZIF-8 capsules on the bulk crystal structure of pristine perovskite.

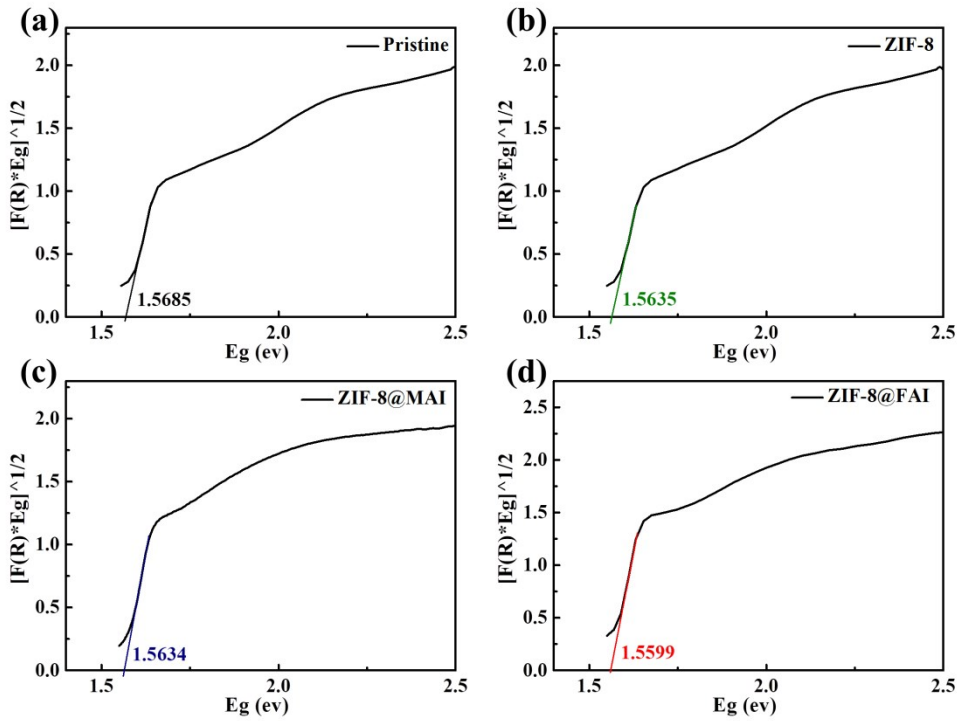

Fig. S5 Optical bandgap estimated based on Tauc plot for (a) Pristine; (b) ZIF-8; (c) ZIF-8@MAI; (d) ZIF-8@FAI.

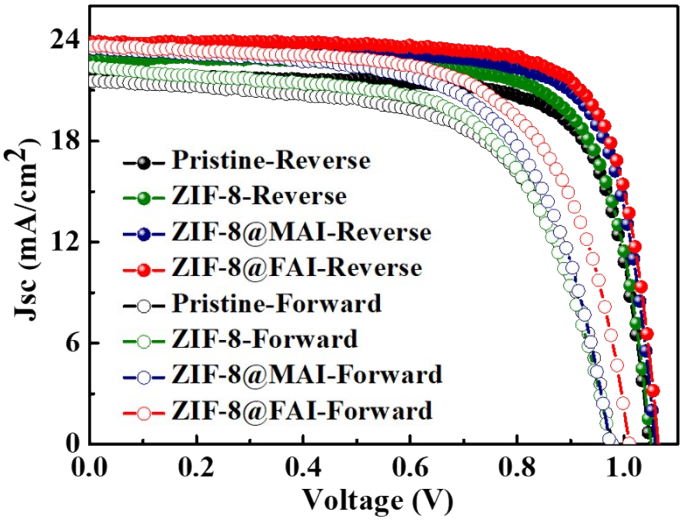

Fig. S6 J–V curves with reverse (1.1 V to −0.2 V) and forward (−0.2 V to 1.1 V) scans of devices.

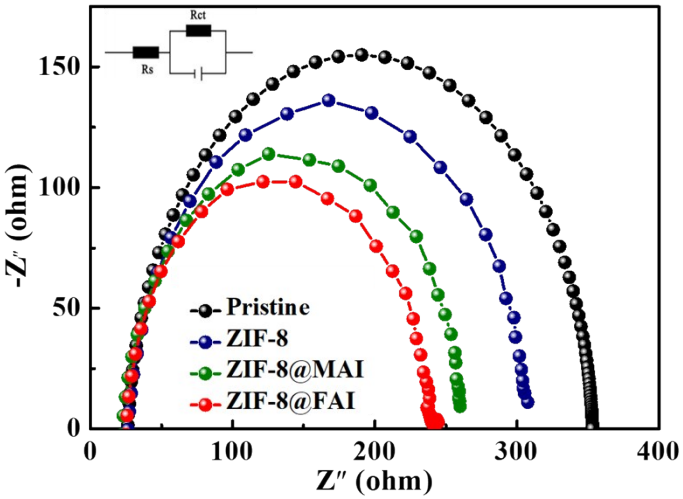

Fig. S7 Electrochemical impedance spectrometry spectra. Inset in is the equivalent circuit.

In order to elucidate the interfacial charge transport behavior in real cell conditions, electrochemical impedance spectroscopy (EIS) measurement was carried out (Fig. S7). The used equivalent circuit model is shown in the inset of Fig. S7, where Rs is the series resistance and Rct is the carrier transport resistance. The Rct of ZIF-8, ZIF-8@MAI, ZIF-8@FAI and Pristine PSCs are 291 Ω, 248 Ω, 193 Ω and 329 Ω, stating the enhanced carrier transport ability with a progressive order of Pristine, ZIF-8, ZIF-8@MAI and ZIF-8@FAI-based PSCs, and the trend is consistent with the SCLC

results.

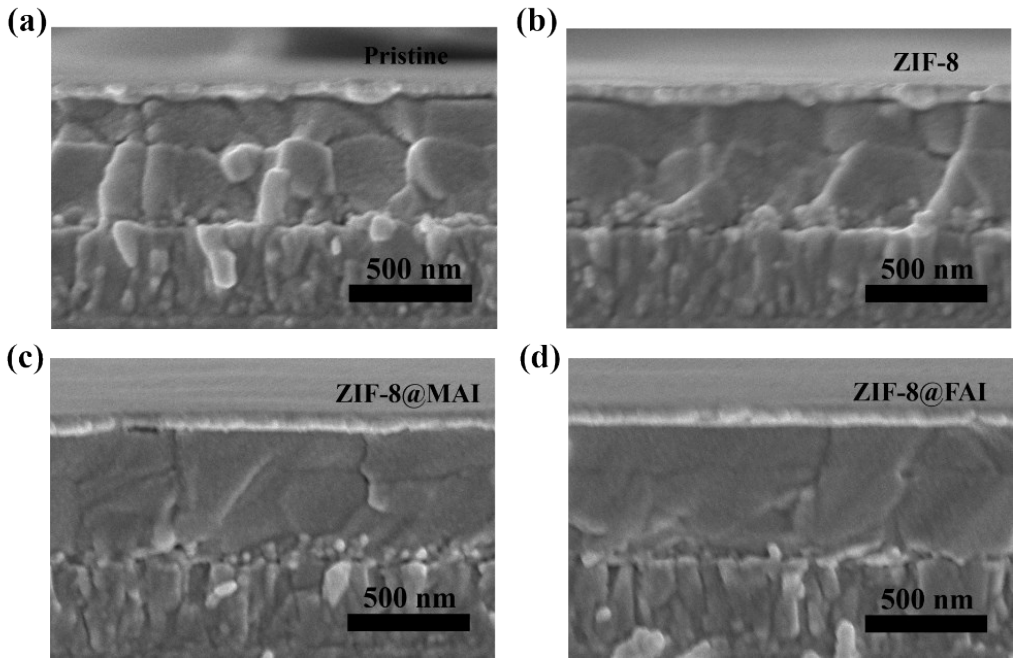

Fig. S8 The cross-sectional SEM images of the devices. (a) Pristine; (b) ZIF-8; (c) ZIF-8@MAI; (d) ZIF-8@FAI.

We fabricate perovskite solar cells based on Pristine, ZIF-8, ZIF-8@MAI and ZIF-8@FAI-based devices, and the cross-sectional SEM images of devices are shown in Fig. S8. Without the incorporation of functional layers (Fig. S8a), the size of perovskite grains is slight less than the thickness of perovskite layers. Therefore, photogenerated charge carriers suffer from the grain boundary scattering in the transport process. After the incorporation of functional layers as shown in Fig. S8b-d, the size of perovskite grains increases and no grain boundary exists in the depth direction. The SEM images also indicate that with the ZIF-8@MAI and ZIF-8@FAI incorporation improves the interface quality between $MAPbI_3$ and Spiro-OMeTAD layers, which can greatly decrease the recombination process of devices.

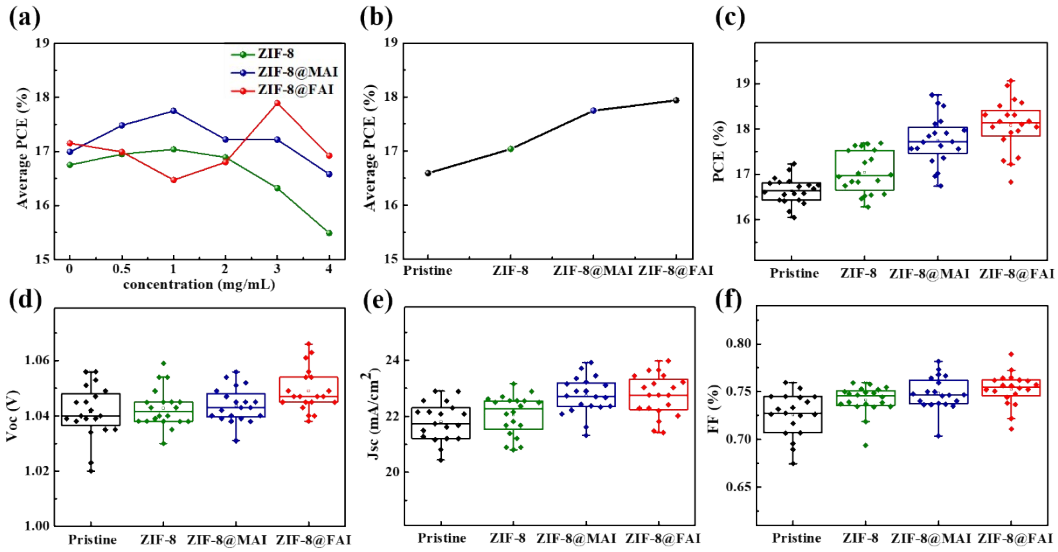

Fig. S9 Photoelectric parameters of the cells. a) Statistical efficiency of the cells in which the perovskite was passivated with varied concentrations of ZIF-8, ZIF-8@MAI and ZIF-8@FAI, respectively; (b) The average efficiency of the optimal concentration of the three passivation materials; (c) The statistical distributions of the PCE parameters; (d) The statistical distributions of the *Voc* parameters; (e) The statistical distributions of the *Jsc* parameters; (f) The statistical distributions of the *FF* parameters.

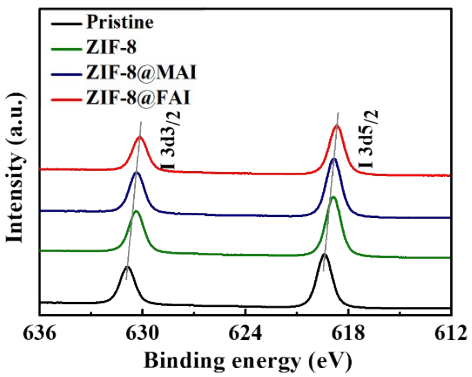

Fig. S10 I3d peaks in XPS spectra.

Figure S10 shows I 3d XPS spectra, where the 3d5/2 and the 3d3/2 peaks are centered at 619.35 eV and 630.82 eV for the pristine device, which is originated from the Pb-I chemical species. The post-treatment shifts the doublet to lower binding energies at 618.84 eV and 630.31 eV for the ZIF-8 device, 618.82 eV and 630.28 eV

for the ZIF-8@MAI device and 618.67 eV and 630.13 eV for the ZIF-8@FAI device. The shift of I 3d peaks to the lower binding energy indicates that oxidation state of iodide is decreased, or the Pb-I bond is weakened by an interaction with MA or FA cation. As shown in Table S3, it should be noted that the I/Pb ratio is higher than the theoretical value of 3, presumably due to the migration of I into the device surface, accelerating its excessive accumulation on the surface. The ratios of I/Pb for pristine perovskite only remained 57% of its initial value (decrease from 3.20 to 1.83) after heating at 80 °C in N_2 for 72 h, revealing the seriously migration of I during the heating process. While the value of perovskite with ZIF-8 treatment increased to 81% (from 3.30 to 2.68) for the suppression of I migration by the ZIF-8 framework. And then, the incorporation of MAI and FAI could further improve the value to 85% and 89%, respectively, displaying the further passivation of the I vacancies.

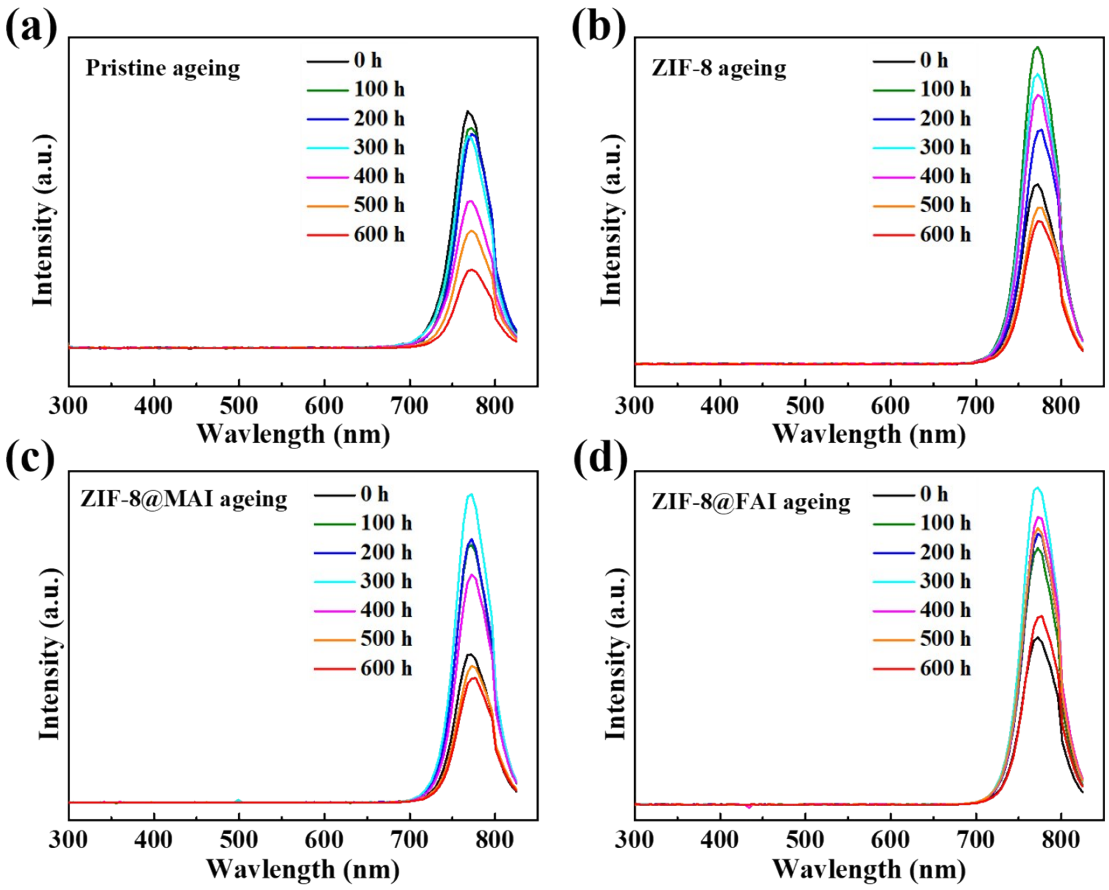

Fig. S11 Evolution of PL intensity stored at room temperature under natural light during 600 h. (a) Pristine; (b) ZIF-8; (c) ZIF-8@MAI; (d) ZIF-8@FAI.

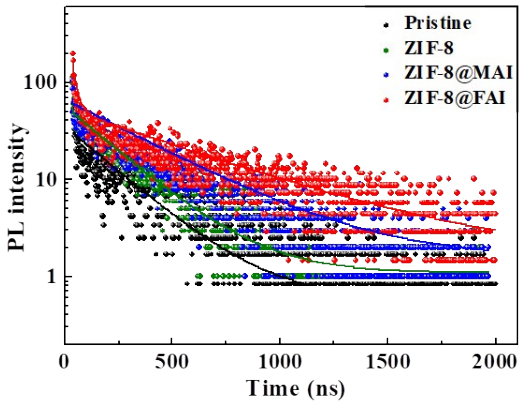

Fig. S12 TRPL spectra of the perovskite films with ZIF-8, ZIF-8@MAI and ZIF-8@FAI modified and pristine.

Based on the TRPL spectra shown in Figure S12, the fitted results for TRPL are summarized in Table S4. We calculated the average lifetime of the perovskite films and found that the lifetime increased from 94.27 to 162.01, 258.90and 272.36 ns for ZIF-8, ZIF-8@MAI and ZIF-8@FAI device, respectively. These results consistently demonstrate that ZIF-8@FAI-based solar cells can attribute to the successful passivation of perovskite defects.

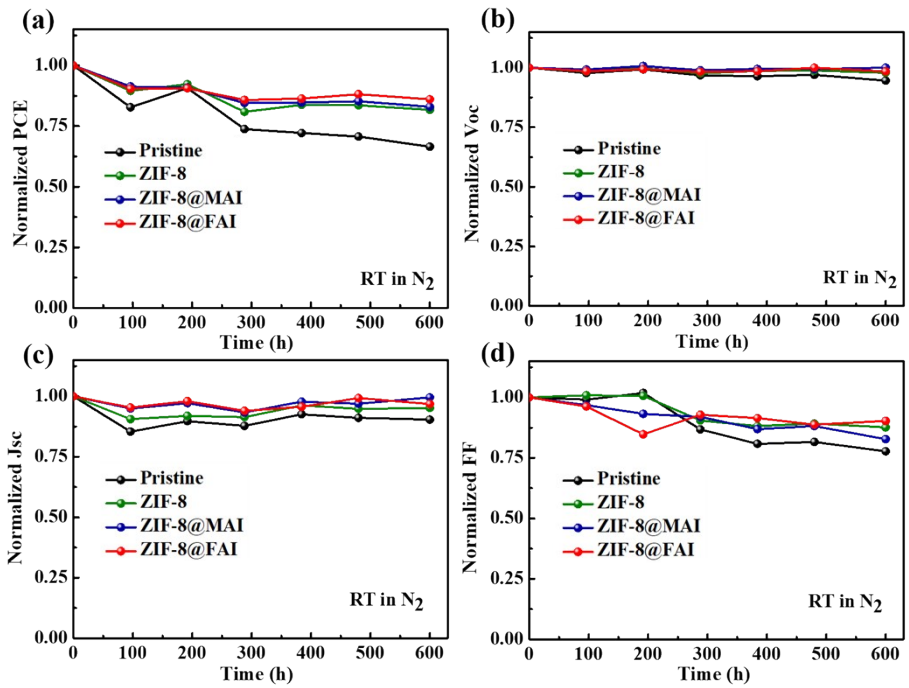

Fig. S13 (a) Long-term stability of PSCs based on different materials (stored temperature about 25 °C in the dark under nitrogen atmosphere for 600 h. (a) *Voc*; (b) *Jsc*; (c) *FF* and (d) PCEs.

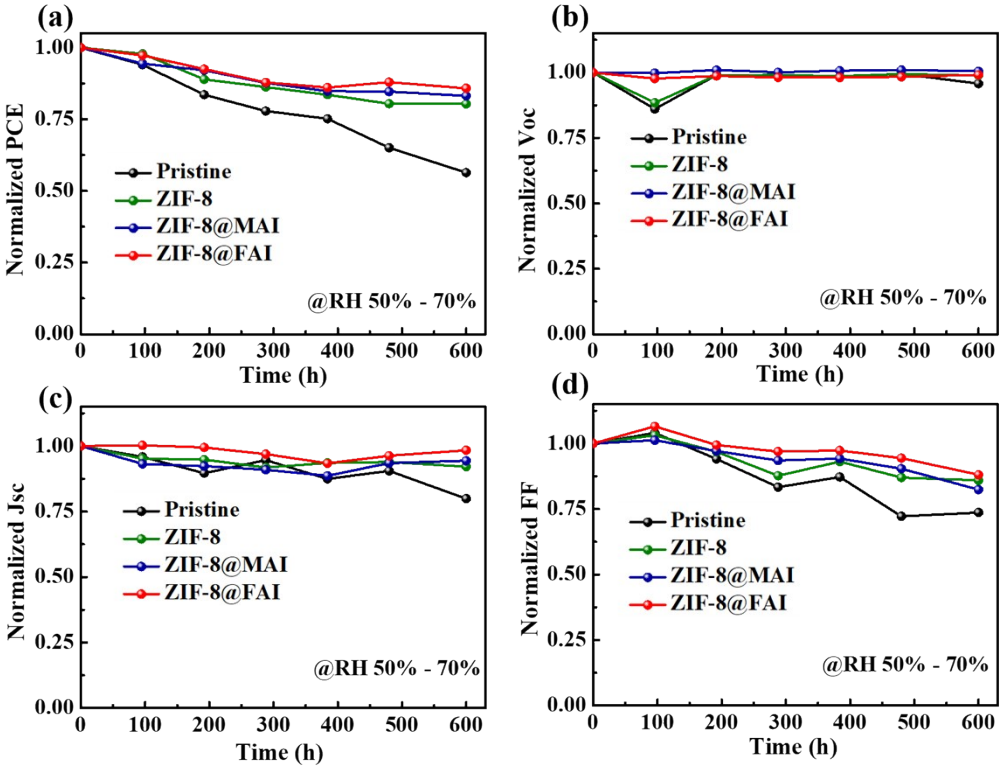

Fig. S14 Long-term stability of PSCs based on different materials (stored conditions: humidity about 50~70 % and temperature about 25 °C in the dark under air atmosphere for 600 h. (a) *Voc*; (b) *Jsc*; (c) *FF* and (d) PCEs.

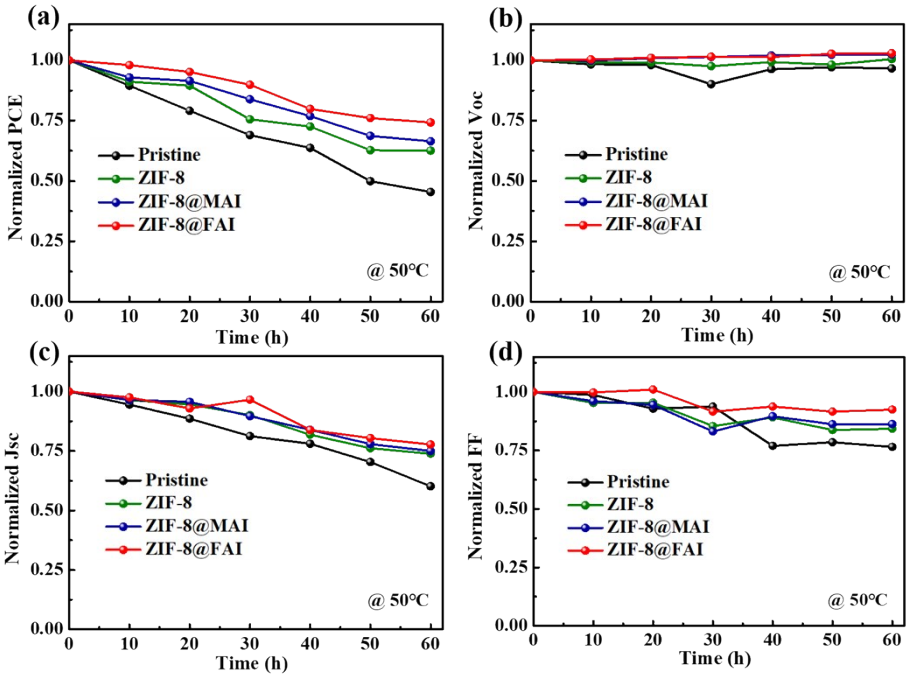

Fig. S15 Thermal stability of PSCs based on different materials (stored contiditions: stored temperature at 50 °C in the dark under nitrogen atmosphere for 600 h. (a) *Voc*; (b) *Jsc*; (c) *FF* and (d) PCEs.

Table S1. Photovoltaics parameters of devices

Devices	Scan direction	*Voc* (V)	*Jsc* (mA/cm^2)	*FF* (%)	PCE (%)	Hysteresis index[a]
Pristine	Reverse	1.047	21.97	74.90	17.23	0.236
	Forward	0.961	22.11	61.9	13.17	
ZIF-8	Reverse	1.048	22.46	75.1	17.69	0.213
	Forward	0.976	22.63	63.0	13.92	
ZIF-8@MAI	Reverse	1.054	23.78	75.2	18.85	0.206
	Forward	0.978	23.89	64.0	14.96	
ZIF-8@FAI	Reverse	1.058	23.93	75.6	19.13	0.187
	Forward	1.007	24.06	64.2	15.55	

a Hysteresis index=($PCE_{reverse}$-$PCE_{forward}$)/$PCE_{reverse}$

Table S2. Resistances values from ZIF-8, ZIF-8@MAI and ZIF-8@FAI devices EIS spectra.

Devices	R_s (Ω)	R_{ct} (Ω)
Pristine	23.7	329
ZIF8	23.4	291
ZIF-8@MAI	19.4	248
ZIF-8@FAI	18.8	193

Table S3. The atomic ratios of pristine, ZIF-8, ZIF-8@MAI and ZIF-8@FAI perovskite films before and after heating at 80 °C for 72 h.

	Pristine		ZIF-8		ZIF-8@MAI		ZIF-8@FAI	
	fresh	aging	fresh	aging	fresh	aging	fresh	aging
Pb (%)	13.88	20.54	13.12	15.63	12.52	14.29	11.22	12.03
N (%)	6.84	2.49	7.08	5.76	7.18	6.37	7.21	6.45
I (%)	44.44	37.5	43.36	41.92	41.55	40.17	37.70	35.86
N/Pb	0.49	0.12	0.54	0.37	0.57	0.45	0.64	0.54
I/Pb	3.20	1.83	3.30	2.68	3.32	2.81	3.36	2.98
N Remain percentage[a]	25%		68%		78%		83%	
I Remain percentage[b]	57%		81%		85%		89%	

a: Remain percentage= (N/Pb(aging))/(N/Pb(fresh))×100%

b: Remain percentage= (I/Pb(aging))/(I/Pb(fresh))×100%

Table S4. The fitting results of the TRPL curves and the films are deposited on glass.

Devices	Rel_1 (%)	τ_1 (ns)	Rel_2 (%)	τ_2 (ns)	τ (ns)
Pristine	56.34	0.53	43.66	215.25	94.27
ZIF-8	28.66	0.97	71.34	226.71	162.01
ZIF-8@MAI	31.29	0.74	68.71	376.47	258.90
ZIF-8@FAI	29.76	0.81	70.24	387.42	272.36